A Feature Tracking Velocimetry algorithm to determine the velocities in Negatively Buoyant Jets

Ferrari Simone[1], Badas M.Grazia[1], Besalduch Luigi A[1]. and Querzoli Giorgio[1]

[1] DICAAR – Dipartimento di Ingegneria Civile, Ambientale e Architettura, University of Cagliari, Italy
ferraris@unica.it

ABSTRACT
We present a novel algorithm, namely Feature Tracking Velocimetry (FTV), which is less sensitive to the appearance and disappearance of particles and to high velocity gradients than classical Particle Image Velocimetry (PIV). The basic idea of FTV is to compare windows only where the motion detection may be successful, that is where there are high luminosity gradients. The FTV algorithm is suitable in presence of different seeding densities, where other techniques produce significant errors, due to the non-homogeneous seeding at the boundary of a flow. The FTV algorithm has been tested for the analysis of laboratory experiments on simple jets (SJs) and negatively buoyant jets (NBJs), both issuing from a sharp-edged orifice. Among the others, the velocity and Turbulent Kinetic Energy profiles, orthogonal to the jet axis, the mean streamwise centerline velocity decay and the integral Turbulent Kinetic Energy along the jet axis have been measured and analyzed. These quantities have been employed to study the differences between simple jets and NBJs, and to investigate how the increase in buoyancy affects the NBJ behavior. Moreover, mean velocity fields have been used to study the geometrical dimensions of the jet, while second order statistics, such as Turbulent Kinetic Energy, have been analyzed to characterize the turbulence structure governing the mixing processes.

Keywords: Feature Tracking Velocimetry (FTV), simple jet, negatively buoyant jet, turbulence.

1. INTRODUCTION

Classical Particle Image Velocimetry (PIV) algorithms obtain velocity fields comparing windows of successive frames on a regular grid in all the image and maximizing the correlation of the light intensity function to obtain their displacement. Typically, PIV is very sensitive to the appearance and disappearance of particles, to high velocity gradients and does not work properly where there are different seeding densities in the investigation field, for instance between a jet and the external fluid, where the seeding cannot be homogeneous. With the target to overcome these issues, we have developed and tested a novel algorithm, namely Feature Tracking Velocimetry (FTV), whose basic idea is to compare windows only where the motion detection may be successful, that is where there are high luminosity gradients.

The FTV algorithm was tested for the analysis of simple jets and negatively buoyant jets (NBJ) issuing from a sharp-edged orifice. While simple jets are generated only by a source of momentum and thus are axisymmetric, inclined NBJs (i.e. released with an angle to the horizontal different from 90°) are generated by a source of both momentum and buoyancy acting in different directions and, consequently, they are non-axisymmetric, due to the different stratifications in the upper and lower boundary (Ferrari and Querzoli 2010 [1] and Ferrari and Querzoli 2011 [2]). There are many practical applications involving NBJs: for instance, the discharges into the sea of brine from desalination plants (e.g. Lai &Lee 2012 [3]), the improvement of water quality by forced mixing in reservoirs, small lakes and harbors (e.g. McClimans & Eidnes 2000 [4]), the forced heating or cooling of large structures such as aircraft hangars, buildings or rooms (e.g. Baines et al. 1989 [5]), etc; see Ferrari & Querzoli (2010) [1] for a detailed list. To the best of authors knowledge, all the previous experimental campaigns on NBJs were performed over NBJs issuing at the end of a long pipe, except for the study of Ferrari & Querzoli (2010) [1], where NBJs were released from a sharp-edged orifice.

Moreover, even most of the experimental campaigns on simple jets carried out during the last decades were on jets issuing from a long pipe or from a convergent nozzle. This has been highlighted, for instance, by Deo et al. (2007) [6], who state that there are very few studies using a plane jet issuing from a sharp-edged orifice-plate, perhaps due to its initial and near-field flow structure being far more complex (e.g. for the existence of a vena contracta). Quinn & Militzer (1988) [7] experimentally and numerically studied a turbulent air jet from a sharp-edged square slot, measuring the mean velocity along the centerline, the turbulent normal and shear stresses (by means of hot-wire anemometry) and the mean static pressure (by means of a pitot-static tube) and found a pronounced mean streamwise velocity off-center peaks in the very near field. Afterwards, Quinn (1989) [8] experimentally compared jets of air issuing from a sharp-edged elliptical and round slot and from a contoured nozzle, finding that sharp-edged slot jets have higher mean streamwise velocity decay rates than contoured nozzle jets, implying higher entrainment and better mixing. Mi et al. (2001) [9] compared mixing performances of three types of nozzle, namely a smooth contraction nozzle, a long pipe

and a sharp-edged orifice, with jets of air with Reynolds number Re = 16,000, finding that the last one provides the greatest rate of mixing. In spite of this performance, also these authors underlined that investigations on circular jets issuing from orifice plates are very limited. A better mixing in a sharp-edged orifice (round and elliptical) jet rather than in a jet from contoured nozzle was found also by Quinn (2006 [10] and 2007 [11]), in his experimental investigation via hot-wire anemometry on jets of air at Re ≅ 180,000. Mi et al. (2007) [12] measured planar velocity using Particle Image Velocimetry (PIV) on a turbulent air jet (Re = 72,000) issuing from a round sharp-edged orifice plate, focusing their efforts on the coherent structures that develop in the near field. Hence, many authors indicate that the sharp-edged orifice is the most effective exit configuration for improving mixing however, those studies were performed at very high Re in order to have unambiguous asymptotic conditions. Indeed, only few studies can be found in literature regarding low Re and/or focusing on the regime of transition to turbulence. Russ and Strykowski (1993) [13] investigated the turbulent structure in the near field of heated jets from a round nozzle as the exit conditions changed from laminar to turbulent. Malmström et al. (1997) [14] measured the streamwise velocity profiles of low-velocity jets from round nozzles of different diameters to examine the dependence of the diffusion of the jet on the outlet conditions.
In order to gain a better knowledge on the behavior of inclined NBJs issuing from a sharp-edged orifice (particularly on the influence of the buoyancy on their behavior) and to test the FTV algorithm on this difficult test case, we present here an experimental investigation on the influence of the densimetric Froude number (the most relevant non-dimensional parameter for NBJs, see chapter 2) on the statistics of velocity fields of simple jets and NBJs, released by a sharp-edged orifice, by means of FTV.

2. DIMENSIONAL ANALYSIS

As stated before, in a NBJ the flow is driven from two sources, one of momentum and one of buoyancy: the first region of the jet is driven mostly by the momentum (so it behaves similarly to a simple jet released with the same angle); far from the outlet, there is a second region where the buoyancy acts to bend the axis down (so the jet behaves similarly to a plume) (List, 1979 [15]). The most relevant non-dimensional parameter for the classification of buoyant jets is the densimetric Froude number, Fr:

$$Fr = \frac{U_0}{\sqrt{g \frac{\rho_{DISC} - \rho_{REC}}{\rho_{REC}} D}}$$

where U_0 is the mean initial jet velocity, g the gravitational acceleration, ρ_{DISC} the discharged fluid density, ρ_{REC} the receiving fluid density and D the outlet diameter. Fr, being the ratio between inertial and buoyancy forces, has low values for heavy jets and high values as buoyancy decreases, up to an infinite value for simple jets.
The other relevant non-dimensional parameters controlling the behavior of inclined NBJs are the Reynolds number, $Re = U_0 D / \upsilon$ (υ is the kinematic viscosity of the discharged fluid), and the angle to the horizontal, θ: as this last parameter controls the misalignment between the flux of buoyancy and the initial flux of momentum, a negatively buoyant jet is axisymmetric only as far as θ is 90°.

3. EXPERIMENTAL SETUP AND FEATURE TRACKING VELOCIMETRY ALGORITHM

The experimental set-up simulates a portion of a pipe laid down on the sea bottom, which discharges the effluent from orifices along the pipe wall, a typical configuration of submarine outfalls. The model consists in a flume with glass walls, filled with water, to simulate a stagnant receiving body. The discharge comes through a pipe, which is connected to a constant head tank, by means of a cylindrical vessel diameter, with a sharp-edge orifice. The released fluid is a solution of water, pollen particles (for the visualization of the jet), to retrieve velocity fields, and sodium sulphate, in case of NBJs, to increase the density. A pumped diode laser illuminates the mean vertical plane of the diffuser, where images are recorded by means of a high speed camera, 400 fps at full spatial resolution (1728×2240). The experiments were performed with a constant flow rate (and high enough to have Re = 1500, larger than its critical value for the apparatus), Fr = 14 ÷ 37.2, θ = 65°. A simple jet (Re = 1500) was experimentally simulated as well for comparison.
Velocity fields were obtained, from each couple of images, using a novel algorithm, namely Feature Tracking Velocimetry (FTV), which is less sensitive to the appearance and disappearance of particles, and to high velocity gradients than classical Particle Image Velocimetry (PIV). PIV algorithms obtain velocity fields comparing windows of successive frames on a regular grid in all the images and minimizing the dissimilarity between the light intensity function to obtain their displacement. The idea of FTV is to compare windows only where the motion detection may be successful, that is where there are high luminosity gradients. The FTV algorithm is suitable in presence of different seeding density, for example between the jet and the external fluid, where other techniques produce significant errors, due to the non-homogeneous seeding at the boundary.
The procedure of analysis consists of:

1. identification of the features using the Harris corner detection (a corner is a region with high luminosity gradients along the x and y direction) (Harris & Stephens, 1988 [16]);
2. ordering of the features according to their corneress (i.e. the value of the Harris formula);
3. selection of the first N features and computation of velocity comparing a window centered with the i^{th} feature (W_t) with windows (W_{t+1}) with a range of displacements, (d_i, d_j) in the next frame;
4. for each displacement a measure of the dissimilarity, $d(d_i, d_j)$, between W_t and $W_{t+1}(d_i, d_j)$ is computed using the Lorentzian estimator; the velocity is obtained as the displacement minimizing the dissimilarity;
5. eventually, samples are validated by means of algorithm based on Gaussian filtering of first neighbors (defined by the Delaunay triangulations), and simulated annealing.

Eventually, samples are validated with the following algorithm based on Gaussian filtering of first neighbors (defined by the Delaunay triangulations), and simulated annealing:

a. for each set of sparse velocity samples the Delaunay triangulation is computed;
b. for each sample, an interpolation of the value of the first neighbors (following the Delaunay triangulation) is computed using a Gaussian weighted average;
c. the difference between the velocity sample and the interpolated value is computed for every sample;
d. if the measured sample giving the larger difference exceeds a given threshold (a parameter of the method), this measured sample is substituted with the interpolation of its neighbors and the steps 2-4 are repeated until all differences are below the threshold.

The statistics of velocity fields are subsequently obtained, by time averaging, under the hypothesis of ergodicity.
The proposed technique is suitable for measurements from a wide range of seeding density: from the high level typical of PIV down to the low seeding which is characteristic of PTV. Additionally, it is suited to the analysis of images with intermediate seeding density or non-homogeneous seeding.
Data from present experiments have been analyzed by means of FTV as well as other classical PIV. The performed comparison shows a good performance of FTV, which provides better results than regular grid based methods especially at shear layer at the border of the jets, leading to sharper fields and more reliable estimation of second order statistics.

4. RESULTS

Here we present the first and second order statistics of the velocity fields to explain the phenomenology of NBJs, to study their geometrical characteristics and, eventually, to highlight the effects of Fr (and, hence, of the buoyancy on jets).
Figure 1 displays the mean velocity field, U, normalized by the maximum velocity at the outlet, U_{MAX}, for a NBJ with Fr = 15, θ = 65°, and Re = 1500. The NBJ covers a very short initial distance, where it maintains a width similar to the diameter of the outlet, afterwards it widens due to the entrainment of surrounding fluid.

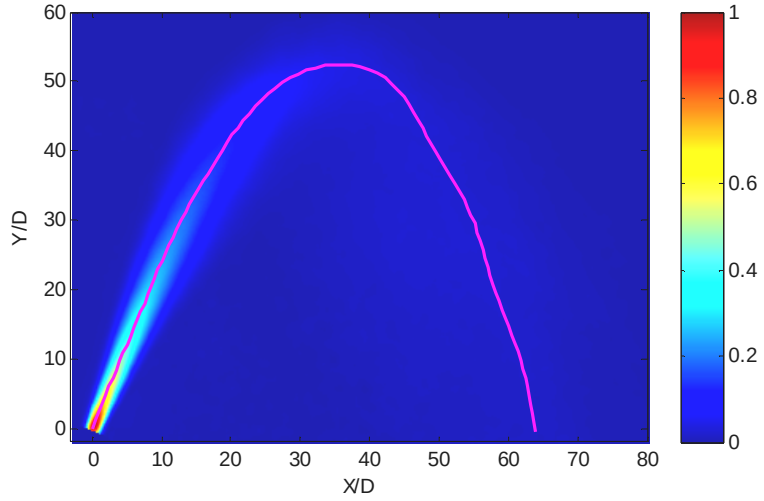

Figure 1 Map of the non-dimensional mean velocity U/U_{MAX} (U_{MAX} is the maximum velocity at the outlet) for a NBJ having Fr = 15, Re = 1500 and a release angle to the horizontal θ = 65°, the pink line represents the jet axis (defined as the locus of maximum intensity velocity).

In Figure 2, profiles of velocity, orthogonal to the jet axis and non-dimensionalised by the axial velocity (U_C), and computed at the same distances along the axis, s/D, are compared for a NBJ with Fr = 14 and θ = 65° and for a SJ with

the same Re = 1500. The plot shows a similar behavior between the two cases for small distances from the origin (s/D = 2), with a symmetrical velocity distribution; vice versa, going further along the axis (s/D = 8, 16), while the velocity profiles of the SJ preserve their symmetry, NBJ ones are asymmetric: in the lower region, the profiles follow the SJ behavior, while in the upper region they tend to widen less than a SJ. Actually, for a NBJ, at the upper boundary the buoyancy acts in the opposite direction to the momentum, allowing the full development of the Kelvin Helmholtz waves, whilst at the lower boundary the buoyancy and momentum act in the same direction, limiting the widening of the profiles.

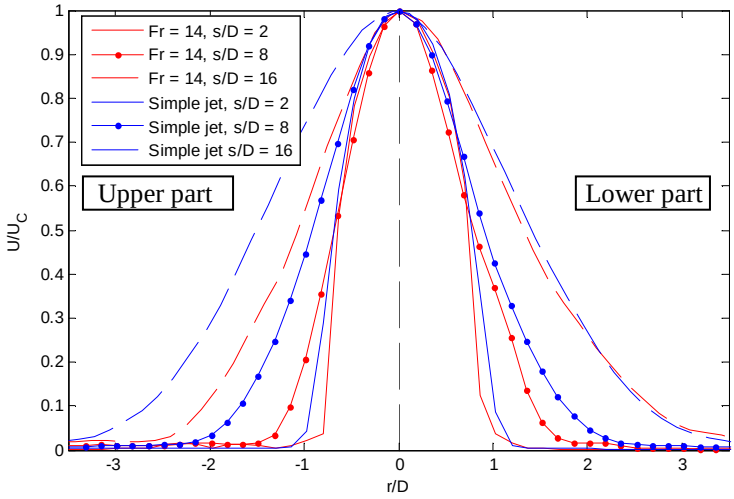

Figure 2. Profiles of velocity, orthogonal to the jet axis and non-dimensionalised by the axial velocity U_C: for a jet with Fr = 14 and θ = 65° (blue lines) and for a simple jet (red lines); Re = 1500; r/D is the orthogonal distance from the axis, s/D is the distance, along the axis, from the origin of the jet.

In order to better show the different behavior of upper and lower NBJ boundaries, Figure 3 shows profiles of velocity, orthogonal to the jet axis and non-dimensionalised by the axial velocity, U_C, for a NBJ with Fr = 15 and θ = 65°. The plot shows how velocity NBJ profiles become more and more asymmetric for larger s/D.

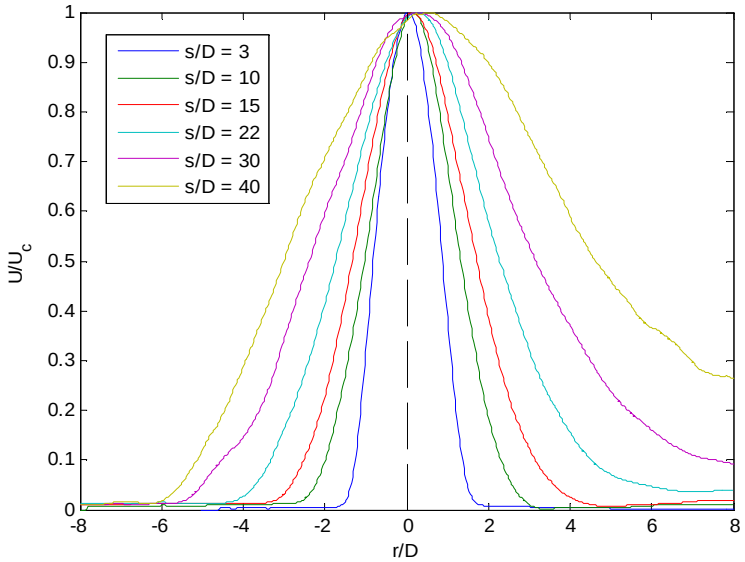

Figure 3. Profiles of velocity, orthogonal to the jet axis and non-dimensionalised by the axial velocity U_C: for a jet with Fr = 15 and θ = 65° (blue lines); Re = 1500; r/D is the orthogonal distance from the axis, s/D is the distance, along the axis, from the origin of the jet.

In Figure 4, the mean velocity profiles $U/U_{C/2}$ are plotted versus $r/r_{1/2}$ for four NBJs (with different Fr), for the simple jet experimental data by Mi 2007 [12], and for the SJ theoretical law by Pope 2000 [17]; $r_{1/2}$ is the jet half width, defined as the r where the velocity assumes the value of $U_{C/2} = U_C / 2$. The equation of Pope is valid far from the jet origin, where the velocity profiles become self-similar:

$$\frac{U}{U_{C/2}} = \frac{1}{\left(1+a\eta^2\right)^2}, \quad \eta = \frac{r}{\left(s-s_0\right)}$$

where s_0 is the virtual origin of the jet, and α is a constant ($\alpha \cong 47$). The NBJ values follow closely both the data of Mi and Pope for all the examined Fr. In this representation, the larger widening of the lower side of NBJs is not apparent due to the normalization of r with $r_{1/2}$ which assumes different values on the upper and lower jet region.

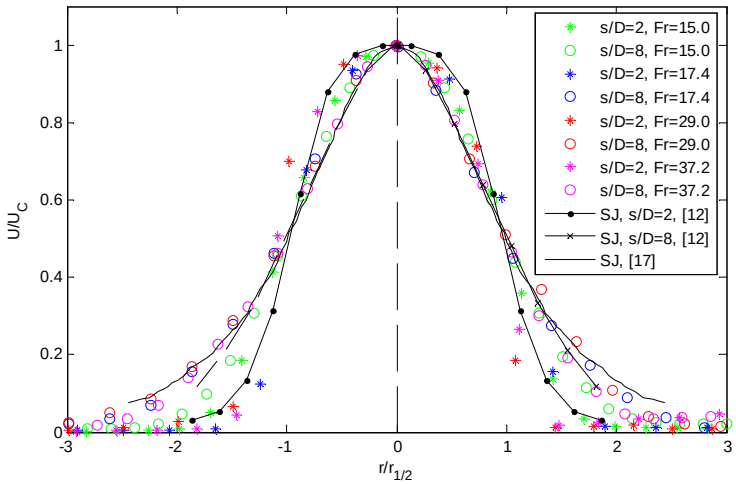

Figure 4. Mean velocity profiles U/U_C, for a NBJ with $\theta = 65°$, Re = 1500 and different Fr (coloured symbols), and for the SJs of Mi 2007 [12] and Pope 2000 [17], (black lines); $r_{1/2}$ is the jet half width.

In Figure 5 we show the widening of a NBJ with Fr = 15, $\theta = 65°$ and Re = 1500 (coloured asterisks) and of the SJs of Quinn 2006 [10] (black rhombi for SJs issuing from a contoured nozzle, black stars for SJs issuing from a sharp-edged orifice). It can be noted that both the NBJ upper and lower boundary grow faster than SJ boundaries. Moreover, it is confirmed that the lower part of NBJs widens more rapidly than the upper one.

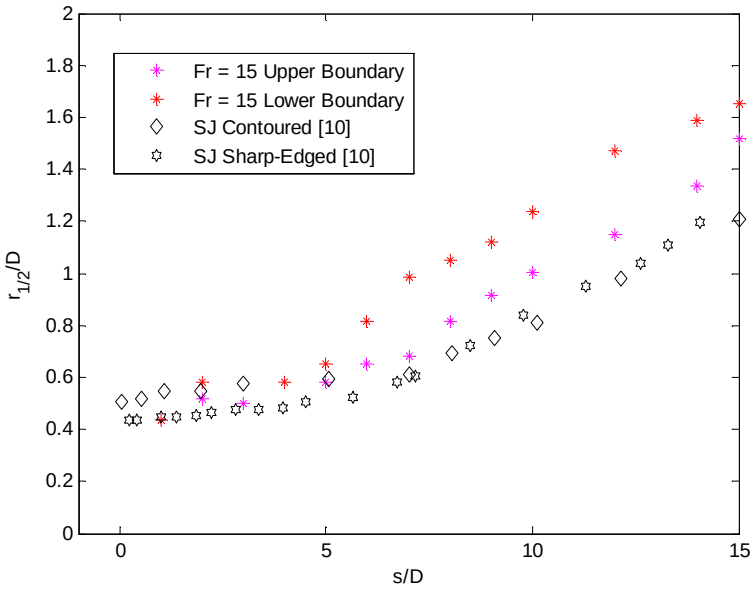

Figure 5. Widening of a NBJ with Fr = 15, $\theta = 65°$ and Re = 1500 (coloured asterisks) and of the SJs of Quinn 2006 [10] (black symbols).

In order to further compare SJs and NBJs, Figure 6 displays the mean streamwise centerline velocity decay, for four NBJs (with different Fr) and for the SJ data by Quinn 2006 [10], issuing from a sharp-edged orifice (black stars) and a contoured nozzle (black rhombi). All the NBJ values display a similar trend to the sharp-edged orifice one, starting with values larger than one due to the vena contracta effect. A dependence on Fr is not apparent on this parameter.

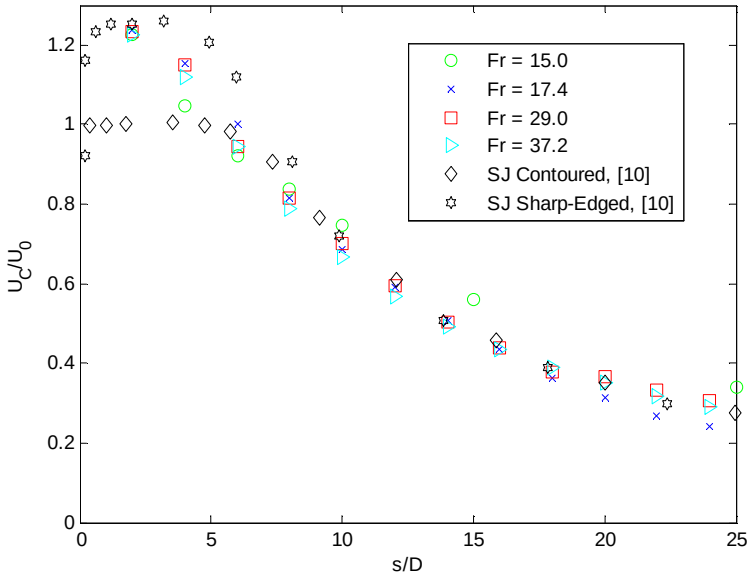

Figure 6. Mean streamwise centreline velocity decay U_C/U_0: for a jet with θ = 65°, Re = 1500 and different Fr (coloured symbols) and simple jets (Quinn 2006 [10], sharp-edged orifice, black stars, and contoured orifice, black rhombi); U_0 is the mean initial jet velocity.

Figure 7a shows the non-dimensional mean Turbulent Kinetic Energy (TKE) field, normalized with U^2_{MAX} for a NBJ with Fr = 15, θ = 65° and Re = 1500: the maximum values are at the jet boundaries, where the turbulence is originated by the Kelvin-Helmholtz billows. To highlight the mentioned asymmetry, in Figure 7b the profiles of TKE, orthogonal to the jet axis and non-dimensionalised with TKE_C (i.e. the axial value on the profile), are presented: there are two peaks at the jet boundaries, with different values, the highest at the upper boundary, the lowest at the lower boundary (with less intense velocity fluctuations due to buoyancy and momentum acting in the same direction). As s/D increases, the two peaks merge into a single peak distribution, with a negative skewness.

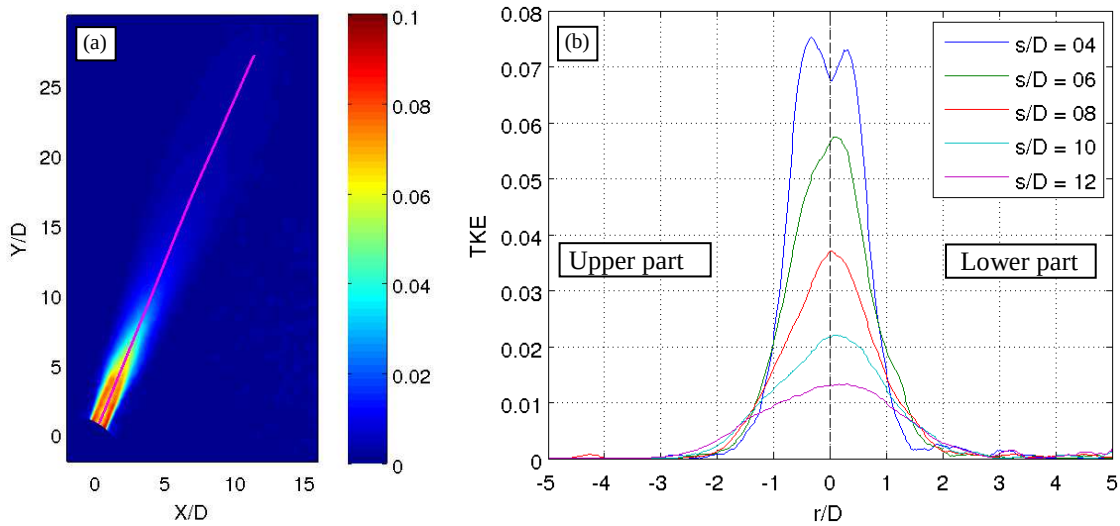

Figure 7. For a jet with Fr = 65°, Re = 1500, θ = 65°: (a) map of the non-dimensional mean turbulent kinetic energy (TKE), non-dimensionalised with U^2_{max}, the pink line represents the jet axis (defined as the locus of maximum velocity), U_{max} is the maximum velocity value; (b) TKE/TKE_C profiles, orthogonal to the jet axis; TKE_C is the axial value on the profile, r/D is the orthogonal distance from the axis, s/D is the distance, along the axis, from the origin of the jet.

In Figure 8, the integral Turbulent Kinetic Energy TKE_{int}/U^2_{max} along the axis is plotted for different Fr and for a SJ (Fr = ∞); U_{max} is the maximum velocity value and the integral is computed on profile orthogonal to the jet axis. The influence of Fr on this parameter is evident: NBJ values start always lower than SJ ones, with an increasing distance with decreasing Fr (i.e., for an increasing buoyancy), to eventually collapse on the SJ values as the distance from the

origin increases. Moreover, the distance where the NBJ data collapse with the SJ ones tends to increase as Fr decreases; this is justified because as Fr decreases, the buoyancy increases, determining a reduction of the turbulent fluctuations.

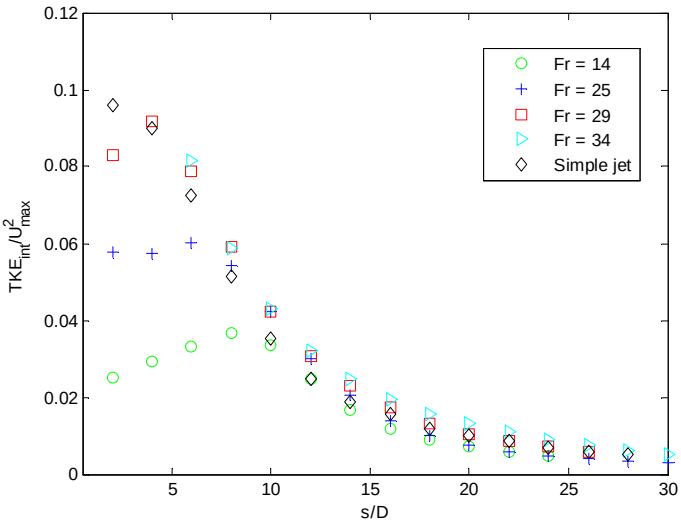

Figure 8. Integral Turbulent Kinetic Energy TKE_{int}/U^2_{max} along the jet axis, for a jet with $\theta = 65°$, Re = 1500 and different Fr (coloured symbols), and for the simple jet (black rhombi) measured with FTV; U_{max} is the maximum velocity value.

As shown above, the analysis on the velocity first order statistics is able to unveil the NBJ non-axisymmetric behavior only at a certain distance from the origin, whilst this characteristic is apparent very close to the origin from the analysis of the velocity second order statistics.

5. CONCLUSIONS

The behavior of inclined Negatively Buoyant Jets, released from a sharp-edged orifice, was investigated using a novel technique to measure the velocity fields, namely Feature Tracking Velocimetry, in order to study their dependence on the densimetric Froude number. First and second order statistics of the velocity fields (velocity and turbulent kinetic energy profiles orthogonal to the jet axis, mean streamwise centerline velocity decay, and integral turbulent kinetic energy along the jet axis) were used to characterize the Negatively Buoyant Jet behavior and their difference from Simple Jets. The analysis of mean velocity fields highlights the different behavior of NBJs with respect to SJs, at a certain distance from the outlet, while velocity second order statistics already unveil the lack of axisymmetry at very short distances from the outlet. Moreover, from the analysis of the second order statistics of the velocity, a dependence of sharp-edged orifice jets on densimetric Froude number is evident.

REFERENCES

1. Ferrari, S. & Querzoli, G. Mixing and re-entrainment in a negatively buoyant jet. Journal of Hydraulic Research, 48(5), 632-640, 2010.
2. Ferrari S. & Querzoli G. Effect of Stable and Unstable Stratification on Negatively Buoyant Jets, Proceedings of 7th Int. Symp. on Stratified Flows, Rome, Italy, August 22 – 26, 2011.
3. Lai, C.C.K. & Lee, J.H.W. Mixing in inclined dense jets in stationary ambient. Journal of Hydro-environment Research, 6, 9-28, 2012.
4. McClimans, T. & Eidnes, G. Forcing nutrients to the upper layer of a fjord by a buoyant plume. Proceedings of the 5th International Symposium on Stratified Flows, Vancouver, 199-204, 2000.
5. Baines, W.D., Turner, J.S. & Campbell, I.H. Turbulent fountains in an open chamber. Journal of Fluid Mechanics. 212, 557-592, 1990.
6. Deo, R.C., Mi, J. & Nathan, G.J. The influence of nozzle-exit geometric profile on statistical properties of a turbulent plane jet. Experimental Thermal and Fluid Science, 32 (2), 545-559, 2007.
7. Quinn, W. R. & Militzer, J. Experimental and numerical study on a turbulent free square jet. Physics of Fluids, 31(5), 1017-1025, 1988.
8. Quinn, W.R. On mixing in an elliptic turbulent jet. Physics of Fluids A, 1(10), 1716-1722, 1989.
9. Mi, J., Nathan, G.J. & Nobes, D.S. Mixing characteristics of axisymmetric free jets from a countered nozzle, an orifice plate and a pipe. Journal of Fluids Engineering, 123, 878-883, 2001.
10. Quinn, W.R. Upstream nozzle shaping effects on near field flow in round turbulent free jets. European Journal of Mechanics B/Fluids, 25, 279–301, 2006.
11. Quinn, W.R.. Experimental study of the near field and transition region of a free jet issuing from a sharp-edged elliptic orifice plate. European Journal of Mechanics B/Fluids, 26, 583-614, 2007.

12. Mi, J., Kalt, P., Nathan, G.J. & Wong, C.Y. PIV measurements of a turbulent jet issuing from round sharp-edged plate. Experiments in Fluids, 42, 625–637, 2007.
13. Russ, S. & Strykowski, P. J. Turbulent structure and entrainment in heated jets: the effect of initial conditions. Physics of Fluids A, 5(12), 3216-3225, 1993.
14. Malmström, T. G., Kirkpatrick, A. T., Christensen, B. & Knappmiller, K. D. Centreline velocity decay measurements in low-velocity axisymmetric jets. Journal of Fluid Mechanics, 246, 363-377, 1997.
15. List, E.J. Turbulent jets and plumes. In: Fisher, H.B., List, E.J., Koh, R.C.Y., Imberger, J. & Brooks, N.H. (Eds). Mixing in inland and coastal water, New York, USA, Academic Press, 315-389, 1979.
16. Harris, C. & Stephens, M. A combined corner and edge detector. In: Proceedings of the 4th Aivey Vision Conference, Manchester, 147-151, 1988.
17. Pope, S.B. Turbulent flows. Cambridge University Press, 771 pp, 2000.